Journal of Bionic Engineering (2022) 19:1589–1600
https://doi.org/10.1007/s42235-022-00224-x

RESEARCH ARTICLE

A Robust Superhydrophobic Smart Coating with Reversible Thermochromic and Photochromic Property

Peng Wang[1,2] · Xuesong Zhang[1,2] · Zhihao Wang[1,2] · Tao Chen[1,2] · Honglian Zhang[1,2] · Wei Duan[1,2] · Huilong Han[1,2]

Received: 20 December 2021 / Revised: 13 May 2022 / Accepted: 18 May 2022 / Published online: 22 July 2022

Abstract
Both thermochromic and photochromic coating have attracted many attentions due to their widely applications, but the low stability is a big obstacle. Inspired by the lotus leaf, to endow the chromic coating with superhydrophobicity is a possible solution. In this research, a dual response coating was prepared by adding photochromic and thermochromic particles simultaneously. The prepared sample demonstrated at least four-state color switching, which can be successfully used in tactile imaging, multi-color fabric, erasable record, and security labels. The superhydrophobicity was achieved by introducing vinyl-terminated polydimethylsiloxane, which not only offers low surface energy but also can cross-link with the particles to increase the adhesion. Thus, the prepared sample maintained superhydrophobicity after various kinds of destruction (such as sandpaper abrasion, corrosive liquid attack, ultrasonic treatment, UV irradiation, and high-speed drops/turbulent jets impact). Even though the superhydrophobicity can be destroyed by plasma etching, it can be recovered after 12 h at room temperature.

Keywords Bionic coating · Superhydrophobic · Thermochromic · Photochromic · Robust

1 Introduction

Chromic coatings which demonstrate a distinctive color change in reply to external stimuli (heat [1, 2], illumination [3], mechanical stress [4, 5], etc.) are attracting more and more attention due to their wide applications in encryptions [6], smart windows [7, 8], display devices [9], and smart fabric [10]. In the past decade, the research on both photochromic and thermochromic materials has made great progress. For instance, Kim et al. [11] synthesized a diarylethenes with a wide range of light response. Hakouk et al. designed a photochromic coating by mixing the photoswitchable cationic spiropyran with polyoxometalate complexes [12]. Marciniak et al. [13] fabricated thermochromic nanomaterials based on Mn^{4+}/Tb^{3+} co-doping. Wang et al. [14] prepared reversible thermochromic nanoparticles consisting of a eutectic mixture. Cataldi et al. [15] combined poly(3-hexylthiophene) with silica to prepare thermochromic superhydrophobic surfaces with high-temperature response and fast color change response. Nevertheless, the coatings demonstrating photochromic and thermochromic properties simultaneously are still rare.

Traditional chromic materials can be easily invaded by water and organic solutions, resulting in degraded performance and corrosion. Then, a potential solution is to further endow the chromic coating with superhydrophobicity. As an ancient Chinese poem says, the lotus rises unstained from the mud. Further research revealed that this excellent self-cleaning performance was due to superhydrophobicity, which has a large contact angle (> 150°) and a little roll-off angle (< 10°) [16–20]. After decades of research, superhydrophobic materials have been widely applied in anti-icing [21, 22], anticorrosion [23], oil–water separation [24], and so on. Recently, some superhydrophobic chromic coatings have been prepared. For instance, Zhang et al. [25] constructed a superhydrophobic and photochromic coating by mixing tungsten oxide and palygorskite, which demonstrated a reversible switching between the colored and discolored states. Zeng et al. [26] reported a superhydrophobic thermochromic film, which shows a reversible color change of blue-pink-yellow by altering the surface temperature. Nevertheless, the mechanical robustness was not reported

✉ Peng Wang
wang.peng.ncepu@foxmail.com

1 School of Energy, Power and Mechanical Engineering, North China Electric Power University, Baoding 071000, China

2 Hebei Key Laboratory of Electric Machinery Health Maintenance and Failure Prevention, North China Electric Power University, Baoding 071003, China

in the aforementioned two references. As the mechanical robustness is the biggest obstacle hindering the superhydrophobic materials' practical application, many methods have been invented. For instance, Parkin et al. [27] introduced an "adhesive + particle" method to improve the interfacial adhesion. Peng et al. [28] prepared all-organic superhydrophobic coatings with mechanical force chemical stability and resistance to liquid permeation by introducing a multiple fluorination strategy. Deng et al. [29] were the first to split superhydrophobicity and mechanical stability into two different structural scales through a decoupling mechanism and proposed the concept of microstructural "armor" to protect superhydrophobic nanomaterials from frictional wear. Chen et al. [30] modified a filamentous hard silica shell on a candle ash template by chemical vapor deposition to enhance the roughness structure and for efficient and robust oil–water separation. Based on this research, making the polymer react with the nanoparticle to form a chemical bond would further improve mechanical robustness.

In this research, both photochromic and thermochromic particles were added. Then, the coating was dual-response which could demonstrate at least four-state color switching. It is found this fast and stable four-state color switching can be used as tactile imaging, multi-color fabric, recording, security labels, etc. The superhydrophobicity was achieved by introducing vinyl-terminated polydimethylsiloxane, which not only offers low surface energy but also cross-link with the particles to increase the adhesion. Thus, the prepared sample maintained superhydrophobicity after various kinds of destruction (such as sandpaper abrasion, corrosive liquid attack, ultrasonic treatment, Ultraviolet (UV) irradiation, and high-speed drops/turbulent jets impact). Even though the superhydrophobicity can be destroyed by plasma etching, it can be recovered after 12 h at room temperature.

2 Experiments

2.1 Materials

Vinyl-terminated polydimethylsiloxane (V-PDMS, viscosity: 1.0×10^5 cP) was purchased from Jucheng Zhaoye Organic Silicone Co., Ltd (China). The vinyltriethoxysilane (VTES, 97%) was provided by Macklin Biochemical Co., Ltd. The silica nanoparticles with a diameter of 10–30 nm were purchased from Huiming Chemical Co., Ltd, China. The three pigments are all organics with a diameter of 1–5 μm (Fig. S1). The digital photos of the color change before and after the response of the pigments (Fig. S2). The FTIR of discolored particles could be found in Fig. S3. The thermochromic pigment A (≤ 31 °C, red; > 31 °C, colorless) and pigment B (≤ 45 °C, green; > 45 °C, colorless) were provided by Ningbo Qiansebian Pigment Co., Ltd. (China). The photochromic pigment C (original, colorless; after UV, blue) were bought from Shenzhen Qianbian Pigment Co., Ltd. More details about the pigments can be found in the supporting information. Ethanol, sodium hydroxide (NaOH), hydrochloric acid (HCl), hexane, and methylene blue were purchased from Aladdin reagent Co., Ltd. (China). All chemicals were used without further purification. Poly(ethylene terephthalate) (PET) fabric (plain weave fabric, density 68×38, 230 g/m^2) was purchased from a local market, which is a polyester of poly(ethylene and terephthalate) (Fig. 2a, b). Before using, it was cleaned by ultrasonic washing with ethanol and deionized water (30 min) sequentially, and then completely dried at 60 °C.

2.2 Preparation of Hydrophobic Suspension

First, 0.15 g silica nanoparticles and 0.5 g V-PDMS were added into 4 g hexane. Then, the mixed solution A was magnetically stirred for 2 h. Separately, 0.08 g pigment A, 0.1 g pigment B, and 0.12 g pigment C were sequentially added into the 10 g VTES under stirring to prepare solution B. In the next step, solution A and B were ultrasonically treated for 10 min to form a uniformly dispersed paint. For the practical application, the materials ratio of the paint was further optimized. The optimized materials ratio can be found in the supporting information.

2.3 Preparation of Superhydrophobic Sample

The superhydrophobic sample could be prepared by either dipping or spray coating. For the dipping, the cleaned fabric was immersed into the hydrophobic paint for 1 h and then baked at 80 °C for 8 h. For the spray coating, the air pressure was set at 0.4 MPa and the distance between the nozzle and sample was 10 cm. After spray coating, the sample was heated at 80 °C for 6 h.

2.4 Characterization

The surface structure of the samples was measured by a scanning electron microscopy (SEM, JSM-IT500). The chemical compositions of the samples were detected using the Fourier transform infrared spectroscopy (FTIR, Nicolet 5700, USA). The water contact angles (CAs) were measured and calculated by a homemade contact angle meter. The water rolling-off angles (RAs) were observed by a high-speed camera (Revealer 2F04). It should be noted that the above CAs and RAs test all used 5 μL water droplets.

3 Results and Discussion

The design concept of this research could be found in Fig. 1a. Three kinds of pigments (1–5 μm diameter, Fig. S1) were utilized to construct a multi-response chromic material. Organic reversible thermochromic materials usually consist of dye, color developer and solvent, also known as ternary

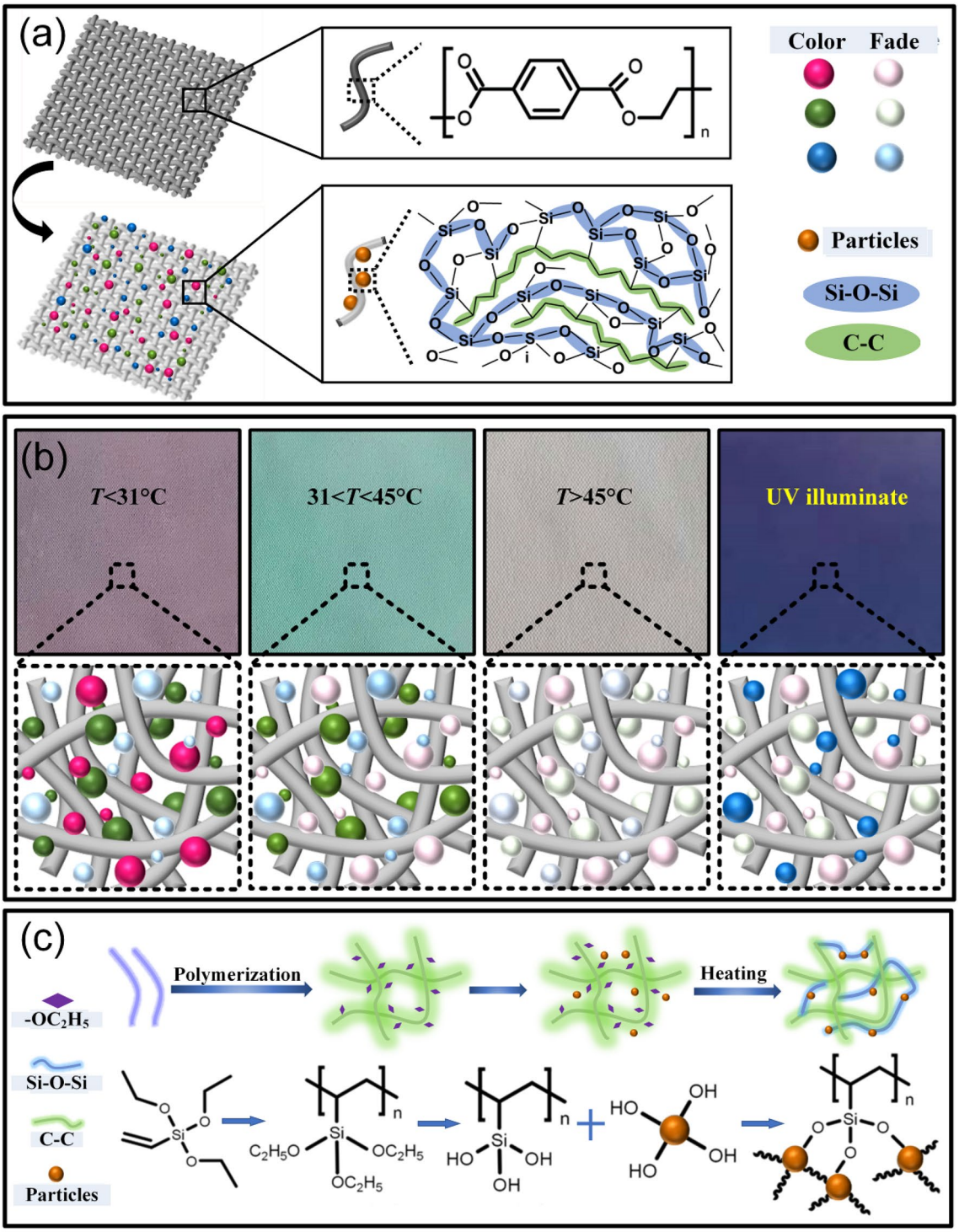

Fig.1 **a** The schematic of multiple chromic responses. **b** Photographs of the prepared sample response to the temperature and UV irradiation. **c** The cross-link mechanism of VTES with particles

complexes. In the present study, melamine–formaldehyde resin was used as the wall material, and the ternary compound composed of dye, developer and solvent was used as the core material. Since the shell of the microcapsules is made of melamine–formaldehyde resin, the microcapsules are well compatible with polysiloxane polymers diluted with *n*-hexane according to the principle of similarity.

Here, pigment A could switch from red to colorless at $T_a = 31$ °C, pigment B could switch from green to colorless at $T_a = 45$ °C, and pigment C could switch from colorless to blue after UV illumination (Fig. 1b). Then, our sample demonstrated four-color states by altering external stimuli. When the external temperature is below 31 °C, the sample exhibited a purple color. When the external temperature is between 31 and 45 °C, a green color could be found on the surface of a sample. When the external temperature is higher than 45 °C, the sample became colorless. After UV irradiation, the sample further changed to blue color.

On this basis, we further tried to endow this chromic sample with superhydrophobicity. After decades of research, it has been proved that the micro/nano structure and low surface energy are two essential factors for preparing superhydrophobicity. Here, the hydrophobic silica nanoparticles were adopted to increase the surface roughness. Recently, the PDMS has been widely used to offer low surface energy [31, 32]. Lai et al. further found heating the PDMS (without a curing agent) at a high temperature help the preparation of superhydrophobic materials [33–36]. In this research, vinyl-terminated PDMS was utilized which not only decrease the surface energy but also increase the durability of the crosslink reaction (Fig. 1c). Here, the small brown sphere represents particles (both chromic and silica particles) with hydroxyl groups on the surface. Under heating conditions, vinyl functional groups in V-PDMS and VTES would polymerize to produce carbon–carbon polymeric structures. Meanwhile, the ethoxy functional group in VTES would hydrolyze and condense with hydroxyl groups in the chromic pigments and hydrophilic silica. This polycondensation not only reduced the hydrophilic groups in the composite but also significantly increased binding between the polymer and the fillers.

The SEM observation was utilized to measure the surface morphology (Figs. 2, 3). Compared with the pristine fabric (Fig. 2a, b), the surface of V-PDMS@ fabric is wrapped by PDMS polymer layer (Fig. 2c, d). Similarly, compared with the V-PDMS@ fabric, the surface of particles-PDMS@ fabric is covered with micro-nano particles wrapped by PDMS polymer layer (Fig. 2e, f). As shown in Fig. 3a, the surface of the fabrics was not smooth. The further high-magnification SEM observations (Fig. 3b, c) revealed that many microscale and nanoscale particles adhere to the fabrics. The microscale particles were recognized as chromic pigments, and the nanoscale particles are ascribed to silica. Moreover, some silica nanoparticles even adhered to the surface of chromic pigments and constructed a hierarchical structure, which facilitates the formation of superhydrophobicity. As reference groups, the surface of original and V-PDMS coated fabrics was smooth (Fig. 2a–d), which further confirmed the contribution of the micro/nanofillers.

Low surface energy is another indispensable element for constructing superhydrophobicity. Here, the surface composition was analyzed using X-ray photoelectron spectroscopy (XPS), FTIR, and energy dispersive spectroscopy (EDS). As displayed in Fig. 4a, only carbon and oxygen elements could be detected from the pristine fabric. However, two distinctive Si 2*p* and 2*s* peaks could be found in the superhydrophobic sample. Moreover, the Si 2*p* peak of superhydrophobic sample demonstrated a much stronger peak than that of pristine fabric (Fig. 4b), indicating that the fabric was well encapsulated by PDMS film. Figure 4c demonstrated the FTIR spectra. It can be found that the pristine fabric demonstrated three main peaks located at 2962 (C–H), 1714 (C=O) and 1258 (Si–C) cm^{-1}, respectively. Compared with pristine fabric, the bending vibrations of Si–C located at 792 cm^{-1} could be found in the superhydrophobic sample with high density, suggesting the V-PDMS was successfully coated onto the fabrics [34]. Moreover, a distinctive peak at 1013 cm^{-1} which was ascribed to Si–O should be explained. Here, the formation of Si–O bond can be ascribed to the hydrolysis and condensation of VTES. Luo et al. found that the hydrolysis of VTES would generate a large amount of –OH groups that are prone to react with each other to form Si–O group [31]. Furthermore, the peaks located at 1628 (C=C) and 1415 (C–H stretching of carbon of vinyl group) cm^{-1} could be found on PDMS@ fabric (Fig. S4). It could be deduced that these two peaks diminished after the cross-linking reaction. The elemental mapping images were further utilized to evaluate the composition distribution. Furthermore, the C, O and Si element were uniformly distributed on the surface of both superhydrophobic sample (Fig. 4d) and PDMS coated fabric (Fig. S5). Thus, it can be deduced that the PDMS was evenly coated onto the fabric, which is in consistent with the XPS and FTIR results.

The most striking feature of smart fabrics is their ability to sense external stimuli and convert them into human-readable signals. Based on dual response (thermochromic and photochromic), our superhydrophobic fabrics have potential applications in erasable fabrics, tactile imaging, writing record, security labels, etc. First, we let a finger contact the sample. Once the heat of the body was transferred to the film, a green fingerprint appeared (Fig. 5a; Movie S1). If no external heat was applied, this fingerprint could exist for more than 5 min. If external heat was applied, this fingerprint would disappear within 10 s. Benefited from the combination of dual response and superhydrophobicity, the water droplet can be used as a non-lossy ink to write

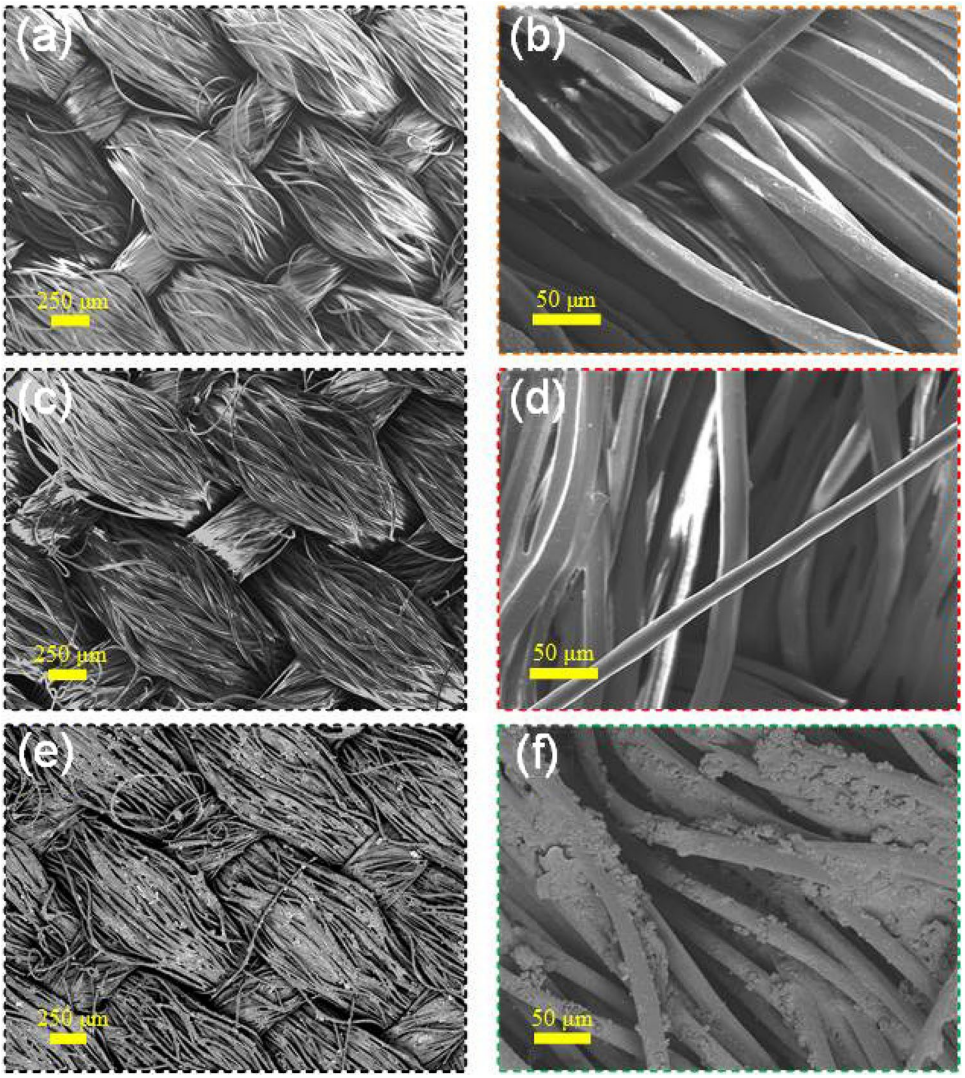

Fig. 2 The SEM of the original fabric (**a**, **b**), V-PDMS@ fabric (**c**, **d**), and particles-PDMS@ fabric (**e**, **f**) at different magnifications

on fabric surfaces. Figure 5b and Movie S2 demonstrate sequential blue letters "1", "2", and "3". Here, the fabric was heated at ~ 38 °C and the temperature of the water droplet was ~ 25 °C. It should be noted that green letters could be obtained if the fabric was put at room temperature and the temperature of the water droplets was between 31 and 45 °C. Based on this stable and reliable discoloration reaction, our fabrics can also be used in transfer printing technology. When a cold template is applied to the surface of the fabric (Fig. 5c; Movie S3), the contact parts changed color, while the noncontact parts remain the original color. Thus, the pattern on the template can be transferred onto the fabric.

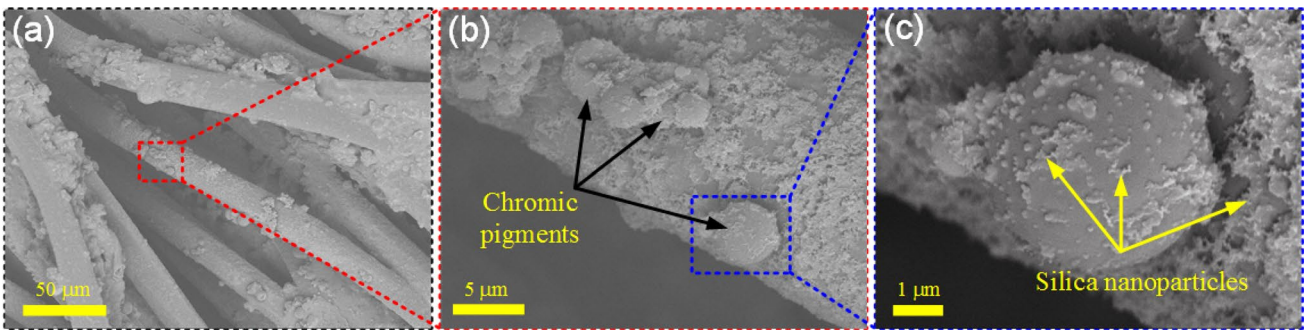

Fig. 3 The SEM images of the superhydrophobic fabrics with different magnifications

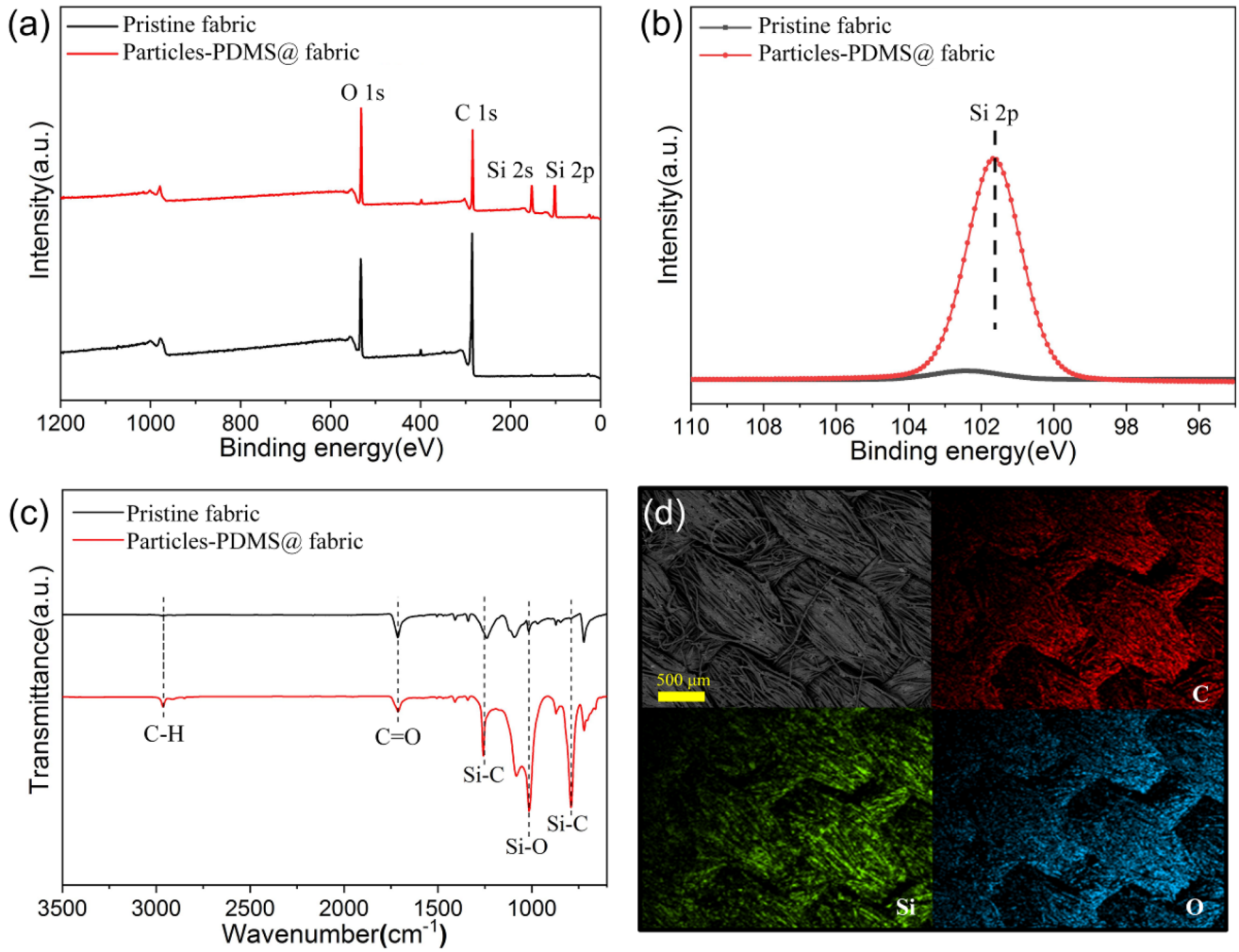

Fig.4 **a** The XPS survey spectra, **b** Si 2*p* spectra and **c** FTIR of the pristine fabric and particles-PDMS@ fabric. **d** Element mapping of particles-PDMS@ fabric

To further extend the application range, the multicolor pattern was prepared by optimizing the filler ratio and regional spraying. A pink flower with green stem can be seen from the fabric at room temperature (Fig. 5d; Movie S4). As the increase of the temperature (31 °C < *T* < 45 °C), the pink flowers gradually disappear. The color could be further changed by ultraviolet irradiation. After the UV treatment at room temperature, a dark blue flower with a dark green stem on the fabric could be prepared. Once the UV treatment was performed at a relative high temperature (31 °C < *T* < 45 °C), a light blue flower and a light green stem could be obtained. Through further structural design and material optimization, our fabrics also have potential applications in anti-counterfeiting labels. As shown in Fig. 4e and Movie S5, a green oblong could be found on the fabric at first. After changing the temperature, the "NCEPU" logo would appear. When further exposing the fabric to ultraviolet light, a "CHINA" logo would appear.

Although the combination of multiple color-changing with superhydrophobicity demonstrated many fascinating properties, the poor durability may hinder its practical applications. First, we quantitatively assess the mechanical robustness. Many methods have been proposed to evaluate the durability of superhydrophobic materials, and the sandpaper abrasion test was the most popular method. Ras et al. further pointed out that the abrasion distance and applied normal pressure were two crucial indicators for the convenience of comparison [37]. Furthermore, some researchers found that the ultrasonic treatment is an effective approach to assess the superhydrophobic textile's durability [34]. Therefore, sandpaper abrasion test and ultrasonic treatment were investigated in the research.

First, commercial sandpaper (Stracke 2000#, Germany) was adopted in the sandpaper abrasion test. The sample was attached to a weight of 1 kg using a double-sided adhesive and moved for 20 cm as one cycle (Movie S6). Although

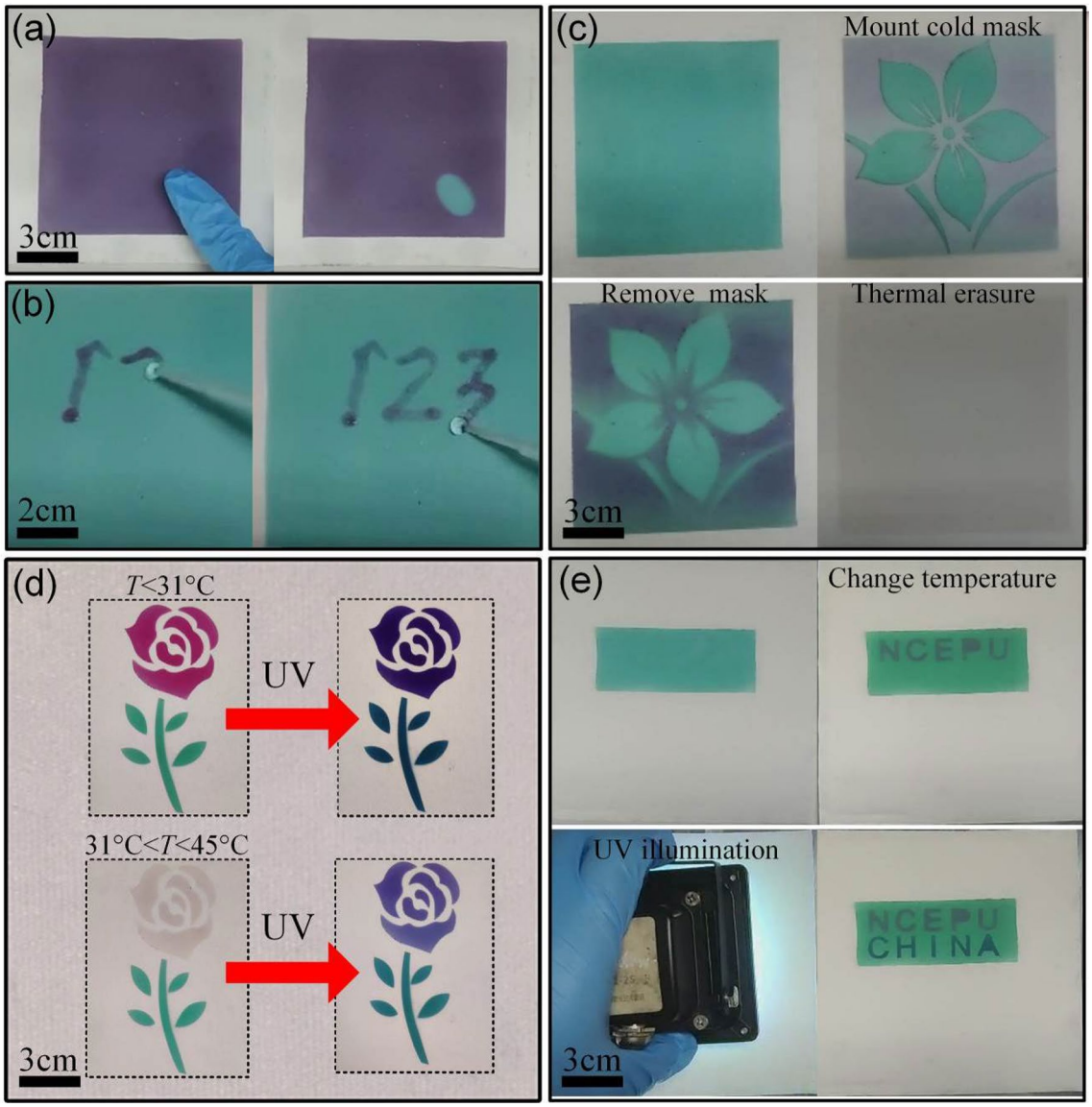

Fig. 5 Photographs of **a** finger touch, **b** writing letters, **c** transfer printing, **d** chromic flower, and **e** anti-counterfeiting label

there are slight repetitions, the overall contact angle keeps getting smaller and the rolling-off angle keeps getting bigger with the increase of abrasion cycles (Fig. 6a). This phenomenon could be ascribed to two reasons: (1) The abrasion abraded some micro/nanofillers attached to the fabrics, and then changed the surface morphology; (2) the abrasion might destroy surface chemistry. Nevertheless, the CAs and SAs were still in the range of superhydrophobicity after 55 abrasion cycles, indicating the relatively strong mechanical robustness (abrasion distance: 11.00 m, applied pressure: 24.90 kPa). From the SEM images after the abrasion test (Fig. S6), it can be found that some micron fibres were worn off, but the intact bodies remained at the junctions of the plain fabric. This means that the fibres can provide a protection to the micro/nano structure consisting of microcapsules and silica, enhancing the stability of the fabric. As a second mechanical robustness test, the sample was put into an ultrasonic bath (80 W, Ningbo Xinzhi Co. Ltd). As shown in Fig. 6b, the effect of ultrasonic treatment on the wettability of fabric is not obvious. The fabric retained excellent superhydrophobic properties even after 24 h of treatment. Thus, it can be deduced that this superhydrophobic textile demonstrated outstanding mechanical robustness. We attributed this to the introduction of V-PDMS, which could generate a cross-linked network between the micro/nanofillers. To fully evaluate the durability, the samples which had been left in the natural environment for 10 months were utilized to withstand sandpaper abrasion, corrosive liquid attack, ultrasnic treatment, UV irradiation, and high-speed drops/turbulent jets impact. The digital photos before and

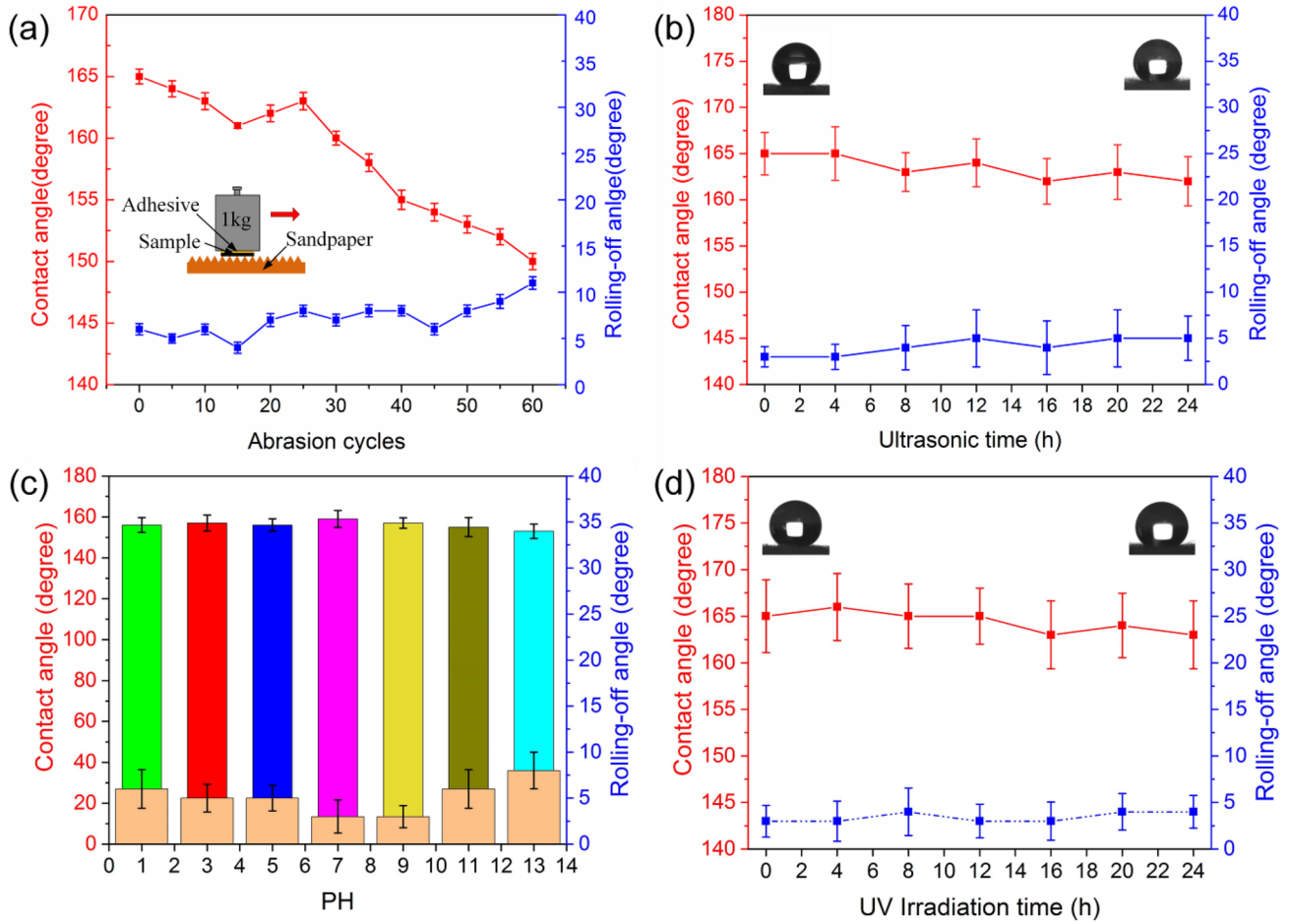

Fig. 6. The CAs and SAs on the superhydrophobic fabrics after **a** sandpaper abrasion, **b** ultrasonic treatment, **c** corrosive liquid attack, and **d** UV irradiation. (The first and last water contact angles of ultrasonic vibration and ultraviolet light are displayed on the corresponding positions)

after the test could be found in Fig. S7. It was worth noting that the water droplets still present a nearly spherical shape on the severely worn area rather than being absorbed by the fabric surface. No visible change in photochromic and thermochromic properties from the pictures. This is mainly attributed to the durability of the microencapsulated shell and the coating effect of V-PDMS. It is speculated that some of these slight variations may be due to partial loss of the coating due to wear.

The chemical durability is another crucial indicator for practical applications. Here, the superhydrophobic textiles were separately immersed aqueous solution with the pH of 1, 3, 5, 7, 9, 11 and 13, respectively. After being immersed in corrosive liquids for 24 h, the sample was rinsed and dried. The further CAs and RAs measurement revealed that the wettability of all the samples was almost unchanged and the superhydrophobicity was retained (Fig. 6c). Furthermore, the superhydrophobic textile might be exposed to sunlight every day. Thus, it is crucial to verify whether it can keep stable under ultraviolet light. Here, we exposed the superhydrophobic net to 10 W UV light and measured

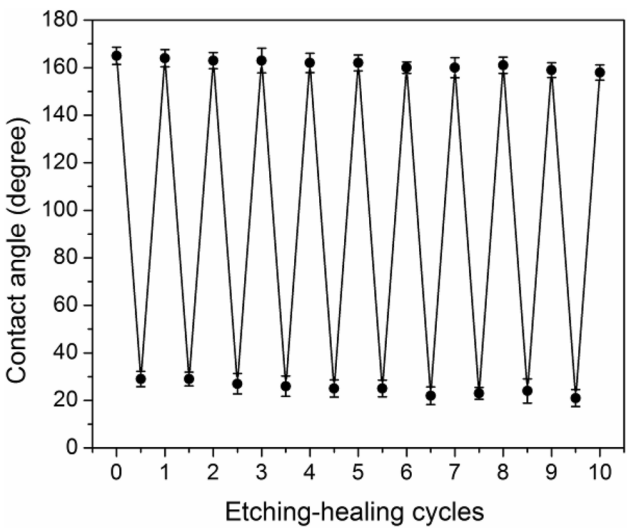

Fig.7 The self-healing cycles of the superhydrophobic fabric after being destroyed by plasma treatment

the CAs and RAs every 2 h. It can be seen that the influence of ultraviolet light on the antenna and rolling angle is negligible (Fig. 6d). We attributed this to the inherent inertness of V-PDMS.

We further investigated the self-healing capability of superhydrophobic textiles. First, the sample was artificially damaged by air plasma. After 1 min of plasma treatment, the superhydrophobic fabrics became hydrophilic with CAs around 30 °C. Lin et al. [38] found that the plasma treatment would introduce a large number of oxygen-containing groups onto the surface. Nevertheless, the superhydrophobicity will be restored after leaving the etched fabrics at room temperature for 12 h. Thus, it can be deduced that the surface of the fabrics becomes hydrophobic again. We attribute this to the excellent hydrophobic mobility of PDMS [39]. The researchers have found that the hydrophobic groups in PDMS tended to spontaneously migrate to the surface (Fig. S8). Moreover, the etching-healing process can be repeated up to 10 times without a significant decrease in the CAs (Fig. 7). Therefore, our superhydrophobic textiles demonstrated outstanding self-healing capability.

The poor resistance to water impact is another important obstacle hindering the superhydrophobic materials' large area industry application. As is well known, the textile such as clothes and textile packaging materials will inevitably encounter stormy weather. Here, we first utilized a high-speed camera to investigate the resistance to droplet impact. Figure S9 demonstrated the repetitive bouncing of an 8 µl droplet on a horizontally placed fabric at an impact velocity of ~ 2.0 m/s, indicating excellent water repellency. For the sake of observation, a tilt angle of 10° was adopted in the later experiment [34]. When the droplet impacted the surface at a relatively low speed (~ 1.0 m/s, Movie S7), it could bounce off rapidly with maintainance of nearly spherical

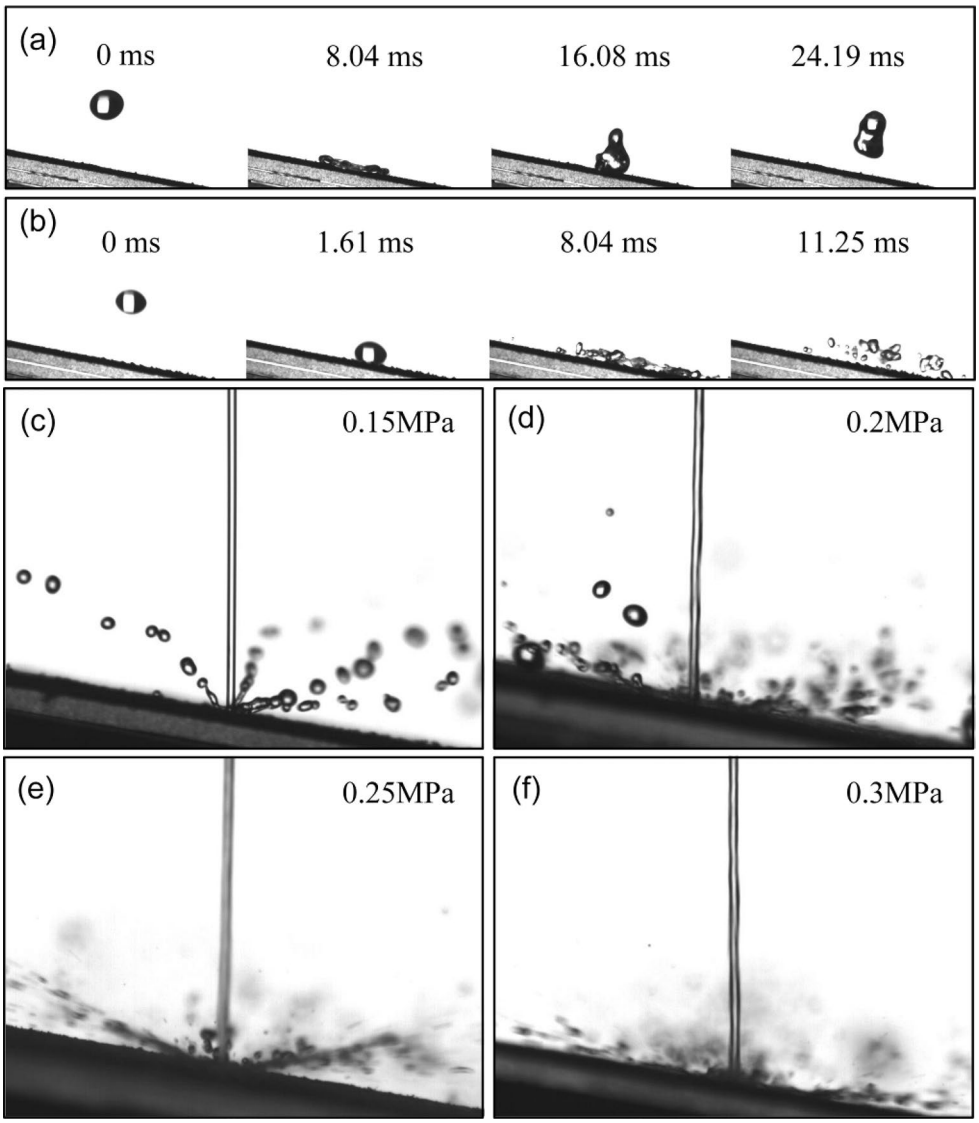

Fig. 8 The typical time-lapse images of a water droplet with the velocity of **a** 1.0 m/s and **b** 3.0 m/s impacting at the surface; The image of water jet test under the pressure of **c** 0.15 MPa, **d** 0.2 MPa, **e** 0.25 MPa and **f** 0.3 MPa

shape (Fig. 8a). When the droplet impacted at a relatively high speed (~ 3.0 m/s, Movie S7), it would splash into many mini-droplets which retained a nearly round shape and rolled off rapidly (Fig. 8b).

To get a higher impact velocity, the pneumatic force was adopted to generate a water jet. Here, we placed the superhydrophobic sample at a tilt angle of ~ 10° and utilized a 1.5 mm diameter nozzle. Then, the resistance to liquid impalement resistance was investigated by subjecting the superhydrophobic sample under different pressure for ~ 5 s as one time. The supporting Movie S8–10 recorded the impact process of one water jet test under the pressure of 0.15, 0.2, 0.25 and 0.3 MPa, respectively. No residue water could be found after the test at the end of the supplementary video. The water droplets rolled off after breaking up on impact, suggesting superhydrophobicity was maintained (Fig. 8c–f). As the pressure increases, it was observed that the droplets rolled down slower. Especially when the pressure is 0.3 MPa, the droplets did not roll off after the impact of the water. The droplet would gradually grow larger and roll off at a certain point, which we believe is similar to the "saturation" phenomenon proposed by Bayer et al. [40]. The increased pressure breaked through the intrinsic microscale of the fabric and the broken droplets remained in the interstices of the micron fibres, resulting in a reduction in superhydrophobicity. However, the recovery of superhydrophobicity only required heating to remove the remaining droplets. The discolored fabric was tested to resist a water flow of 0.25 MPa without saturation and showed excellent recovery (Fig. S10). We attributed this to the very small water droplets from the water impact which entered the fabric without damaging the microscale structure consisting of the PDMS-coated fabric fibres [41]. Moreover, the superhydrophobic textile could withstand the impact of water jet for more than 10 times. As Tiwari al. has claimed that the softness helps improve impact resistance [28], the introduction of V-PDMS could soften the fabric and then enhance the resistance to water impalement.

4 Conclusion

In summary, we have developed a dual-response superhydrophobic chromic coating with robust mechanical robustness and self-healing capability. The coatings were prepared by a combination of photochromic particles, thermochromic particles and vinyl-terminated polydimethylsiloxane. Due to the rapid and highly reversible four-state color switching, this superhydrophobic textile can be successfully applied in tactile imaging, writing a record, multi-colored textile, and security label. It should be noted that the polydimethylsiloxane in this research not only offers low surface energy but also cross-link with the particles to increase the adhesion. Thus, the prepared sample maintained superhydrophobicity after various kinds of destruction (such as sandpaper abrasion, corrosive liquid attack, ultrasonic treatment, UV irradiation, and high-speed drops/turbulent jets impact). Even though the superhydrophobicity can be destroyed by plasma etching, it can be recovered after 12 h at room temperature.

Supplementary Information The online version contains supplementary material available at https://doi.org/10.1007/s42235-022-00224-x.

Acknowledgements This work was supported by the National Nature Science Foundation of China (51977079, 51607067), the Central Guidance on Local Science and Technology Development Fund of Hebei Province (226Z1204G), the Top Young Innovative Talents of Colleges and universities of Higher Learning Institutions of Hebei (BJ2021095), Youth Elite Scientists Sponsorship Program by the Chinese Society for Electrical Engineering (CSEE-YESS-2017002), and the Fundamental Research Funds for the Central Universities (2020MS115, 2017MS149).

Data Availability Statement Data available on request from the authors.

Declarations

Conflict of interest The authors declare that they have no conflict of interest.

References

1. Chae, S., Lee, J. P., & Kim, J. M. (2016). Mechanically drawable thermochromic and mechanothermochromic polydiacetylene sensors. *Advanced Functional Materials, 26*, 1769–1776.
2. Galliani, D., Mascheroni, L., Sassi, M., Turrisi, R., Lorenzi, R., Scaccabarozzi, A., Stingelin, N., & Beverina, L. (2015). Thermochromic latent-pigment-based time-temperature indicators for perishable goods. *Advanced Optical Materials, 3*, 1164–1168.
3. Zhang, Y. J., Yang, H. Y., Ma, H. L., Bian, G. F., Zang, Q. G., Sun, J. W., Zhang, C., An, Z. F., & Wong, W. Y. (2019). Excitation wavelength-dependent fluorescence of an ESIPT triazole derivative for amine sensingand anti-counterfeiting applications. *Angewandte Chemie International Edition, 58*, 8773–8778.
4. Zeng, S. S., Zhang, D. Y., Huang, W. H., Wang, Z. F., Freire, S. G., Yu, X. Y., Smith, A. T., Huang, E. Y., Nguon, H., & Sun, L. Y. (2016). Bio-inspired sensitive and reversible mechanochromisms via strain-dependent cracks and folds. *Nature Communications, 7*, 11802.

5. Gao, X. Y., & Guo, Z. G. (2017). Biomimetic superhydrophobic surfaces with transition metals and their oxides: A review. *Journal of Bionic Engineering, 14*, 401–439.
6. Zhu, Q. D., Vliet, K. V., Holten-Andersen, N., & Miserez, A. (2019). A double-layer mechanochromic hydrogel with multidirectional force sensing and encryption capability. *Advanced Functional Materials, 29*, 1808191.
7. Banisadr, S., Oyefusi, A., & Chen, J. (2019). A versatile strategy for transparent stimuli-responsive interference coloration. *ACS Applied Materials & Interfaces, 11*, 7415–7422.
8. Lin, J., Lai, M. L., Dou, L. T., Kley, C. S., Chen, H., Peng, F., Sun, J. L., Lu, D., Hawks, S. A., Xie, C. L., Cui, F., Alivisatos, A. P., Limmer, D. T., & Yang, P. D. (2018). Thermochromic halide perovskite solar cells. *Nature Materials, 17*, 261–267.
9. Kim, G., Cho, S., Chang, K., Kim, S. W., Kang, H., Ryu, S. P., Myoung, J., Park, J., Park, C., & Shim, W. (2017). Spatially pressure-mapped thermochromic interactive sensor. *Advanced Materials, 29*, 1606120.
10. Wei, Y. F., Zhang, W., Hou, C. Y., Zhang, Q. H., Li, Y. G., & Wang, H. Z. (2021). Independent dual-responsive Janus chromic fibers. *Science China-Materials, 64*, 1770–1779.
11. Jeong, W., Khazi, M. I., Park, D. H., Jung, Y. S., & Kim, J. M. (2016). Full color light responsive diarylethene inks for reusable paper. *Advanced Functional Materials, 26*, 5230–5238.
12. Matsubara, K., & Tatsuma, T. (2007). Morphological changes and multicolor photochromism of Ag nano particles deposited on single-crystalline TiO_2 surfaces. *Advanced Materials, 19*, 2802–2806.
13. Piotrowski, W., Trejgis, K., Maciejewska, K., Ledwa, K., Fond, B., & Marciniak, L. (2020). Thermochromic luminescent nanomaterials based on Mn^{4+}/Tb^{3+} codoping for temperature imaging with digital cameras. *ACS Applied Materials & Interfaces, 12*, 44039–44048.
14. Shen, S., Feng, L., Qi, S. Y., Cao, J., Ge, Y. R., Wu, L., & Wang, S. (2020). Reversible thermochromic nanoparticles composed of a eutectic mixture for temperature-controlled photothermal therapy. *Nano Letters, 20*, 2137–2143.
15. Cataldi, P., Bayer, I. S., Cingolani, R., Marras, S., Chellali, R., & Athanassiou, A. (2016). A thermochromic superhydrophobic surface. *Scientific Reports, 6*, 27984.
16. Ebrahimi, M., Bayat, A., Ardekani, S. R., Iranizad, E. S., & Moshfegh, A. Z. (2021). Sustainable superhydro phobic branched hierarchical ZnO nanowires: Stability and wettability phase diagram. *Applied Surface Science, 561*, 150068.
17. Khan, S. A., Boltaev, G. S., Iqbal, M., Kim, V. V., Ganeev, R., & Alnaser, A. (2021). Ultrafast fiber laser-induced fabrication of superhydrophobic and self-cleaning metal surfaces. *Applied Surface Science, 542*, 148560.
18. Abad, S. N. K., Ilkhechi, N. N., Adel, M., & Mozammel, M. (2020). Hierarchical architecture of a superhy drophobic Cd–Si co-doped TiO_2 thin film. *Applied Surface Science, 533*, 147495.
19. Wang, P., Chen, T., Zhang, X. S., Duan, W., Zhang, C. Y., Han, H. L., & Xie, Q. (2021). A superhydrophobic hydrogel for self-healing and robust strain sensor with liquid impalement resistance. *Chinese Journal of Chemistry, 39*, 3393–3398.
20. Wang, P., Wei, W. D., Li, Z. Q., Duan, W., Han, H. L., & Xie, Q. (2020). A superhydrophobic fluorinated PDMS com posite as a wearable strain sensor with excellent mechanical robustness and liquid impalement resistance. *Journal of Materials Chemistry A, 8*, 3509–3516.
21. Wang, P., Yao, T., Li, Z. Q., Wei, W. D., Xie, Q., Duan, W., & Han, H. L. (2020). A superhydrophobic/electrothermal synergistically anti-icing strategy based on graphene composite. *Composites Science and Technology, 198*, 108307.
22. Wang, P., Li, Z. Q., Xie, Q., Duan, W., Zhang, X. C., & Han, H. L. (2021). A passive anti-icing strategy based on a su perhydrophobic meshwith extremely low ice adhesion strength. *Journal of Bionic Engineering, 18*, 55–64.
23. Milles, S., Soldera, M., Kuntze, T., & Lasagni, A. F. (2020). Characterization of self-cleaning properties on superhydrophobic aluminum surfaces fabricated by direct laser writing and direct laser interference patterning. *Applied Surface Science, 525*, 146518.
24. Nguyen, H. H., Tieu, A. K., Wan, S. H., Zhu, H. T., Sang, P. T., & Johnston, B. (2021). Surface characteristics and wettability of superhydrophobic silanized inorganic glass coating surfaces textured with a picosecond laser. *Applied Surface Science, 537*, 147808.
25. Dong, J., & Zhang, J. P. (2019). Photochromic and super antiwetting coatings based on natural nanoclays. *Journal of Materials Chemistry A, 7*, 3120–3127.
26. Su, X. J., Li, H. Q., Lai, X. J., Zheng, L. Z., Chen, Z. H., Zeng, S. S., Shen, K. Y., Sun, L. Y., & Zeng, X. R. (2020). Bioinspired duper hydrophobic thermochromic films with robust healability. *ACS Applied Materials and Interfaces, 12*, 14578–14587.
27. Lu, Y., Sathasivam, S., Song, J. L., Crick, C. R., Carmalt, C. J., & Parkin, I. P. (2015). Robust self-cleaning surfaces that function when expose to either air or oil. *Science, 347*, 1132–1135.
28. Peng, C. Y., Chen, Z. Y., & Tiwari, M. K. (2018). All-organic superhydrophobic coatings with mechanochemical robustness and liquid impalement resistance. *Nature Materials, 17*, 355–360.
29. Wang, D. H., Sun, Q. Q., Hokkanen, M. J., Zhang, C. L., Lin, F. Y., Liu, Q., Zhu, S. P., Zhou, T. F., Chang, Q., He, B., Zhou, Q., Chen, L. Q., Wang, Z. K., Ras, R. H. A., & Deng, X. (2020). Design of robust superhydrophobic surfaces. *Nature, 582*, 55–59.
30. Chen, B. Y., Zhang, R. R., Fu, X. H., Xu, J. D., Jing, Y., Xu, G. H., Wang, B., & Xu, H. (2022). Efficient oil–water separation coating with robust superhydrophobicity and high transparency. *Scientific Reports, 12*, 2187.
31. Liu, M. L., Luo, Y. F., & Jia, D. M. (2020). Polydimethylsiloxane-based superhydrophobic membranes: Fabrication, durability, repairability, and applications. *Polymer Chemistry, 11*, 2370–2380.
32. Li, Y. S., Ren, M., Lv, P. F., Liu, Y. Z., Shao, H., Wang, C., Tang, C. Y., Zhou, Y. L., & Shuai, M. B. (2019). A robust and flexible bulk superhydrophobic material from silicone rubber/silica gel prepared by thiol-ene photopolymerization. *Journal of Materials Chemistry A, 7*, 7242–7255.
33. Xie, X. W., Li, S. H., Wang, X. Q., Huang, J. Y., Chen, Z., Cai, W. L., & Lai, Y. K. (2021). An effective and low-consumption foam finishing strategy for robust functional fabrics with on-demand special wettability. *Chemical Engineering Journal, 426*, 131245.
34. Zhu, T. X., Cheng, Y., Huang, J. Y., Xiong, J. Q., Ge, M. Z., Mao, J. J., Liu, Z. K., Dong, X. L., Chen, Z., & Lai, Y. K. (2020). A trans parent superhydrophobic coating with mechanochemical robustnessfor anti-icing, photocatalysis and self-cleaning. *Chemical Engineering Journal, 399*, 125746.
35. Gao, S. W., Dong, X. L., Huang, J. Y., Li, S. H., Li, Y. W., Chen, Z., & Lai, Y. K. (2018). Rational construction of highly trans parent superhydrophobic coatings based on a non-particle, fluorine-free and water-rich system for versatile oil-water separation. *Chemical Engineering Journal, 333*, 621–629.
36. Ge, M. Z., Cao, C. Y., Liang, F. H., Liu, R., Zhang, Y., Zhang, W., Zhu, T. X., Yi, B., Tang, Y. X., & Lai, Y. K. (2020). A "PDMS-in-water" emulsion enables mechanochemically robust superhydrophobic surfaces with self-healing nature. *Nanoscale Horizons, 5*, 65–73.
37. Tian, X. L., Verho, T., & Ras, R. H. A. (2016). Moving superhydrophobic surfaces toward real-world applications. *Science, 352*, 142–143.
38. Zhou, H., Wang, H. X., Niu, H. T., Gestos, A., & Lin, T. (2013). Robust, self-healing superamphiphobic fabrics preparedby two-step coating of fluoro-containing polymer, fluoroalkyl silane, and

modified silica nanoparticles. *Advanced Functional Materials, 23*, 1664–1670.
39. Xue, C. H., Bai, X., & Jia, S. T. (2016). Robust, self-healing superhydrophobic fabrics prepared by one-step coating of PDMS and octadecylamine. *Scientific Reports, 6*, 27262.
40. Bayer, I. S., Davis, A. J., Loth, E., & Steele, A. (2015). Water jet resistant superhydrophobic carbonaceous films by flame synthesis and tribocharging. *Materials Today Communications, 3*, 57–68.
41. Cai, R. G., Glinel, K., Smet, D. D., Vanneste, M., Mannu, N., Kartheuser, B., Nysten, B., & Jonas, A. M. (2018). Environmentally friendly super-water-repellent fabrics prepared from water-based suspensions. *ACS Applied Materials and Interfaces, 10*, 15346–15351.
42. Su, X. J., Li, H. Q., Lai, X. J., Zhang, L., Wang, J., Liao, X. F., & Zeng, X. R. (2017). Vapor-liquid sol-gel approach to fabricating highly durable and robust superhydrophobic polydimethylsiloxane@silica surface on polyester textile for oil-water separation. *Applied Materials and Interfaces, 9*, 28089–28099.